A Model of the Stimulation of a Nerve Fiber by Electromagnetic Induction

BRADLEY J. ROTH AND PETER J. BASSER

Abstract—**A model is presented to explain the physics of nerve stimulation by electromagnetic induction. Maxwell's equations predict the induced electric field distribution that is produced when a capacitor is discharged through a stimulating coil. A nonlinear Hodgkin–Huxley cable model describes the response of the nerve fiber to this induced electric field. Once the coil's position, orientation, and shape are given and the resistance, capacitance, and initial voltage of the stimulating circuit are specified, this model predicts the resulting transmembrane potential of the fiber as a function of distance and time. It is shown that the nerve fiber is stimulated by the gradient of the component of the induced electric field that is parallel to the fiber, which hyperpolarizes or depolarizes the membrane and may stimulate an action potential. Finally, it predicts complicated dynamics such as action potential annihilation and dispersion.**

INTRODUCTION

IN the last decade a novel method of nerve stimulation has been developed which exploits the principle of electromagnetic induction [1], [2]. This technique has been used to map the motor cortex [3]–[5] and measure central motor conduction delay in patients with multiple sclerosis [6]–[8] and degenerative ataxic disorders [9]. It has also been used to measure conduction velocity in peripheral nerves [10]. Stimulation by electromagnetic induction is noninvasive and less painful than applying a voltage difference to surface electrodes. In practice, stimulation is effected by passing a time-varying current through a wire coil that is in close proximity to excitable tissue (Fig. 1). Although many investigators have demonstrated this phenomenon experimentally in both peripheral nerves and the cerebral cortex, a physical description of the interaction between the induced electric field and these excitable tissues has not yet been elucidated.

In this paper we present a model combining elementary circuit analysis, Maxwell's equations of electromagnetic theory, and nonlinear cable theory to explain the action of the induced electric field upon a nerve fiber. The current source and stimulating coil are modeled as a series RLC circuit. The induced electric field distribution within the tissue is calculated from the geometry of the stimulating coil and the time course of the current. The effect of the induced electric field upon the nerve is determined with a cable model which contains active Hodgkin–Huxley elements. Inputs to the model are physical properties of the nerve fiber such as its membrane capacitance and conductance, and independent variables such as the coil geometry, its position and orientation with respect to the nerve fiber, and the capacitance and initial voltage of the stimulating circuit. The model then predicts the resulting transmembrane potential in the fiber as a function of distance and time. There are no free parameters in this description of the interaction of the electromagnetic field and the nerve fiber.

Manuscript received March 23, 1989; revised July 27, 1989.

The authors are with the Biomedical Engineering and Instrumentation Branch, Division of Research Services, National Institutes of Health, Bethesda, MD 20892.

IEEE Log Number 9034755.

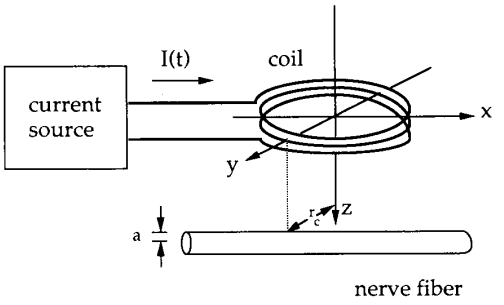

Fig. 1. A schematic diagram showing the experimental apparatus for stimulating a nerve using electromagnetic induction. A current $I(t)$ is passed through a coil placed near a nerve fiber; the induced electric field stimulates the nerve. The nerve lies parallel to the x axis at $y = r_c$ and $z = 1.0$ cm. The coil radius is also r_c; the fiber radius is a.

It is shown that the magnitude and time-course of the gradient of the component of the induced electric field parallel to the nerve fiber determines whether stimulation occurs, and where it occurs. This quantity plays a similar role in electromagnetic stimulation as the applied transmembrane current density plays in nerve stimulation by a microelectrode. It can hyperpolarize or depolarize the membrane and can stimulate the fiber to propagate an action potential.

THEORY

Passive Cable Model

In this section we develop a mathematical model of the action of electromagnetic induction on a passive nerve fiber, appropriate for describing its subthreshold behavior. We employ the cable equation to model the passive properties of a nerve fiber [Fig. 2(a)] [11], [12]. The underlying assumptions of this model are: 1) the intracellular potential is only a function of the axial distance x (i.e., the distance along the length of the fiber) [13]; 2) the

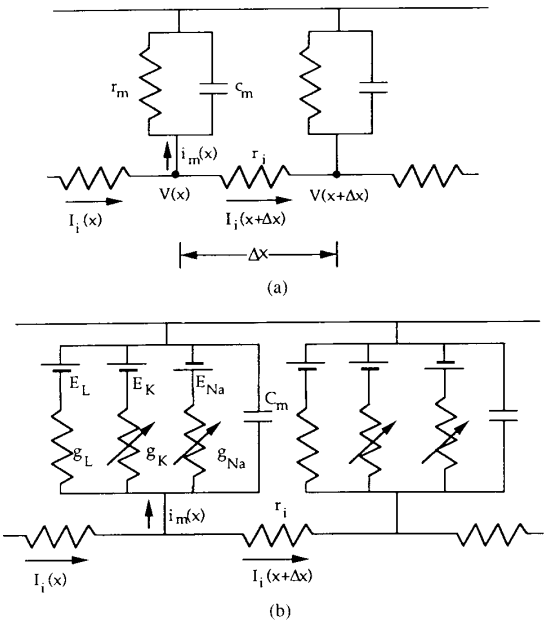

Fig. 2. (a) An electrical circuit representing the passive cable. The intracellular space is modelled by a resistance per unit length r_i, the membrane by a resistance times unit length r_m and capacitance per unit length by c_m. The extracellular potential is assumed to be zero. The axial intracellular current $I_i(x)$ is related to the intracellular potential $V(x)$ by Ohm's law, and related to the membrane current per unit length, $i_m(x)$ by the equation of continuity. (b) An active cable with Hodgkin–Huxley membrane. The membrane is now represented by three voltage and time dependent conductances, representing the sodium, potassium, and leakage channels [22].

axoplasm behaves like a linear, Ohmic conductor whose resistance per unit length is r_i; and 3) the extracellular potential produced by the fiber's own activity is negligible. The last assumption is also used by Rattay in his model of electrical stimulation using extracellular electrodes [14], and is valid because the extracellular potential produced by an action potential propagating along a single nerve axon lying in a large extracellular volume conductor is less than 1 mV [15]. This assumption would not be valid for a nerve surrounded by a thin layer of conducting fluid suspended in air or oil. Because we can neglect the extracellular potential, the intracellular potential can be set equal to the transmembrane potential V.

Referring to Fig. 2(a), we see that the axial current inside the fiber I_i is given by Ohm's law

$$r_i I_i = -\frac{\partial V}{\partial x} \tag{1}$$

and the membrane current per unit length i_m is given by the law of conservation of current

$$i_m = -\frac{\partial I_i}{\partial x}. \tag{2}$$

The passive membrane is represented by a capacitance per unit length of c_m and a resistance times unit length of r_m. The membrane current per unit length is therefore given by

$$i_m = c_m \frac{\partial V}{\partial t} + \frac{V}{r_m}. \tag{3}$$

These three equations can be combined to yield the familiar cable equation

$$\lambda^2 \frac{\partial^2 V}{\partial x^2} - V = \tau \frac{\partial V}{\partial t} \tag{4}$$

where the length constant λ is

$$\lambda = \sqrt{\frac{r_m}{r_i}} \tag{5}$$

and the time constant τ is

$$\tau = c_m r_m. \tag{6}$$

So far we have only considered the contribution to the intracellular electric field that arose from the charge distribution on the membrane's surface. In that case, we were justified in equating the axial component of the electric field inside the fiber E_i with the negative gradient of the intracellular potential

$$E_i = -\frac{\partial V}{\partial x}. \tag{7}$$

However, in electromagnetic stimulation a time-varying magnetic field gives rise to an additional source of electric field through electromagnetic induction. Therefore, (7) must be amended to include the component of the induced electric field parallel to the fiber $\epsilon_x(x, t)$:

$$E_i = -\frac{\partial V}{\partial x} + \epsilon_x(x, t). \tag{8}$$

The induced electric field equals the negative rate of change of the magnetic vector potential $\boldsymbol{A}$

$$\boldsymbol{\varepsilon} = -\frac{\partial \boldsymbol{A}}{\partial t}. \tag{9}$$

It is important to realize that the induced electric field cannot be expressed as the gradient of the voltage, but instead must be related to a vector potential [16]. Both the vector potential and induced electric field are determined by the coil current and geometry [17], as we describe in detail below. We also note that it is the component of the electric field parallel to the fiber (in the axial direction) that enters our model and ultimately results in stimulation of the nerve. This is consistent with the conclusion of Rushton [18] that electric fields oriented parallel to nerve fibers cause stimulation more readily than electric fields oriented transverse to fibers.

Taking (8) into consideration, (1) must be rewritten as

$$r_i I_i = -\frac{\partial V}{\partial x} + \epsilon_x(x, t). \tag{10}$$

Equation (2), which follows from the continuity of current, remains valid. In principle, (3) should be modified to take into account the radial component of ε in the membrane. However, the strength of the electric field in the membrane due to charge on its surface is on the order of 10^7 V/m whereas the electric field strength induced in the tissue by the coil is generally less than 10^3 V/m. Therefore, we can safely neglect the contribution of ε to the membrane current. When we combine (2) and (3) with (10), we obtain a modified cable equation

$$\lambda^2 \frac{\partial^2 V}{\partial x^2} - V = \tau \frac{\partial V}{\partial t} + \lambda^2 \frac{\partial \epsilon_x}{\partial x} \tag{11}$$

where λ and τ are the same space and time constants defined above. The new term in the cable equation acts like a sink of transmembrane potential, with a strength proportional to the axial derivative of the induced electric field and the square of the length constant. This result is analogous to the conclusion of Rattay [14], [19], [20], who considered stimulation of nerve fibers by distant electrodes.

The reason that the derivative of the electric field appears in (11) instead of the electric field itself is because the membrane current, not the axial current along the fiber, depolarizes the membrane. By (2) we see that the membrane current is a maximum where the spatial gradients of the axial current and the induced electric field are the largest. Interestingly, at the location along the fiber where the electric field is maximum the axial derivative of the electric field must necessarily be zero, so we expect little or no stimulation to occur where the electric field is largest. This conclusion is in contrast to the assertion by Barker *et al.* that stimulation occurs where the electric field is maximum [6], but is consistent with the recent observation by Reilly that a spatial gradient of the electric field is required for stimulation [21].

Hodgkin-Huxley Model

While the passive cable model provides insight into the way the induced electric field interacts with the nerve, it does not completely describe the dynamics of nerve stimulation. In order to study the stimulation and propagation of action potentials, we must consider an active membrane model. We use the Hodgkin-Huxley model [22] to represent the nerve membrane.

To implement the Hodgkin-Huxley model, we modify the passive cable model [Fig. 2(b)]. The resistance per unit length of the fiber r_i can be expressed in terms of the fiber radius a and the resistivity of the axoplasm R_i as $r_i = R_i/\pi a^2$. The membrane current per unit length i_m is related to the membrane current density J_m by the expression $i_m = 2\pi a J_m$; similarly the membrane capacitance per unit length c_m is related to the capacitance per unit area C_m by $c_m = 2\pi a C_m$. Finally, we replace the membrane resistance times unit length r_m by an active model of the time and voltage dependent sodium, potassium, and leakage channels [22] [Fig. 2(b)]. With these modifications, the cable equation becomes

$$\frac{a}{2R_i}\frac{\partial^2 V}{\partial x^2} - \left(g_{\mathrm{Na}} m^3 h (V - E_{\mathrm{Na}}) + g_{\mathrm{K}} n^4 (V - E_{\mathrm{K}}) + g_L (V - E_L) \right) = C_m \frac{\partial V}{\partial t} + \frac{a}{2R_i}\frac{\partial \epsilon_x}{\partial x}(x, t) \tag{12}$$

where g_{Na}, g_{K} and g_L are the peak sodium, potassium, and leakage membrane conductances per unit area, and E_{Na}, E_{K}, and E_{L} are the sodium, potassium, and leakage Nernst potentials. The gating variables m, h, and n are dimensionless functions of time and voltage which vary between zero and one. Each gating variable follows a first-order differential equation

$$\frac{\partial m}{\partial t} = \alpha_m (1 - m) - \beta_m m \tag{13}$$

$$\frac{\partial h}{\partial t} = \alpha_h (1 - h) - \beta_h h \tag{14}$$

$$\frac{\partial n}{\partial t} = \alpha_n (1 - n) - \beta_n n \tag{15}$$

where the α's and β's are voltage dependent rate constants determined from voltage clamp measurements

$$\alpha_m = \frac{0.1[-40 - V]}{\exp\left(\frac{-40 - V}{10}\right) - 1.0} \tag{16}$$

$$\beta_m = 4.0 \exp\left(\frac{-65 - V}{18}\right) \tag{17}$$

$$\alpha_h = 0.07 \exp\left(\frac{-65 - V}{20}\right) \tag{18}$$

$$\beta_h = \frac{1.0}{\exp\left(\frac{-35 - V}{10}\right) + 1.0} \tag{19}$$

$$\alpha_n = \frac{0.01[-55 - V]}{\exp\left(\frac{-55 - V}{10}\right) - 1.0} \tag{20}$$

$$\beta_n = 0.125 \exp\left(\frac{-65 - V}{80}\right) \tag{21}$$

(We have assumed that the resting potential is -65 mV; V is measured in mV, α and β in ms^{-1}.)

Equations (12) through (21) constitute a system of four, nonlinear, coupled partial differential equations. They are solved numerically for the transmembrane potential $V(x, t)$ and the three gating parameters $m(x, t)$, $n(x, t)$, and $h(x, t)$, using the method of lines. In this technique, the fiber is subdivided into a discrete number of intervals in which the trial solution is approximated by a summation of functions of x multiplied by functions of t. By requiring that these solutions are continuous at each node, it is possible to transform this system of partial differential equa-

tions into a system of first-order, ordinary differential equations in t which can be solved using Gear's method.

It is assumed that the membrane is initially at rest, i.e.,

$$\frac{\partial V}{\partial t} = \frac{\partial m}{\partial t} = \frac{\partial h}{\partial t} = \frac{\partial n}{\partial t} = 0 \qquad \text{for } t = 0. \quad (22)$$

The transmembrane voltage is taken to be its resting value; m, n, and h are each assigned their asymptotic values, m_∞, n_∞, and h_∞, respectively, evaluated at the resting potential [22]. The boundary conditions applied at $x = \pm L$, far from the region where the stimulus strength is large, are that the axial gradients in the transmembrane potential and the three gating parameters vanish,

$$\frac{\partial V}{\partial x} = \frac{\partial m}{\partial x} = \frac{\partial h}{\partial x} = \frac{\partial n}{\partial x} = 0 \qquad \text{for } x = \pm L. \quad (23)$$

Equations (12)–(21) were solved on a VAX 750 (D.E.C., MA) using programs written in Fortran which made use of several IMSL scientific subroutines, including MOLCH (Version 10, TX).

The model parameters given in Table I are the same ones Hodgkin and Huxley used in their model of the squid giant axon. The temperature of the fiber is taken as $T = 18.5$ C (the same temperature that Hodgkin and Huxley used in several simulations), and a Q_{10} of 3 was used to convert the expressions for the rate constants from 6.3 to 18.5 C [22]. While we contend that many of the qualitative features of nerve conduction in humans are represented in the Hodgkin–Huxley model, we do not claim that our results are applicable to humans quantitatively. In order to model the dynamics of a mammalian peripheral nerve, the fiber radius, temperature and gating kinetics would have to be modified to account for the differences in electrical properties between mollusks and mammals. Moreover, the Hodgkin–Huxley model is developed for an unmyelinated nerve, whereas most of the larger peripheral nerves in mammals are myelinated and propagate action potentials by saltatory conduction.

The Electric Field Produced by a Coil

To complete our model, we must calculate the electric field induced by a time-varying current in the coil. Maxwell's equations provide the relationship between the electric field and the coil current. We assume the problem can be treated in the quasistatic limit, thereby ignoring effects of electromagnetic wave propagation [23]. Cohen and his colleagues [17] have shown that the induced electric field ε can be calculated from the coil current and its geometry by

$$\varepsilon(\boldsymbol{r}, t) = \left(\frac{dI(t)}{dt}\right)\left(-\frac{\mu_0 N}{4\pi}\int \frac{d\boldsymbol{l}'}{|\boldsymbol{r} - \boldsymbol{r}'|}\right) \quad (24)$$

where μ_0 is a constant ($4\pi \times 10^{-7}$ V s/Am), N is the number of turns in the coil, $I(t)$ is the coil current, $\boldsymbol{r}$ is the position where the electric field is calculated, and $\boldsymbol{r}'$ is the position of the differential element of the coil $d\boldsymbol{l}'$. The induced electric field is separable; it can be expressed as the product of a function of time and a function of space. Once the coil geometry has been prescribed, the spatial distribution of the electric field can determined independently of the current from the integral in (24). We consider a circular coil with $N = 30$ turns having a radius of 2.5 cm. Following Cohen *et al.* [17], we approximate this coil as a 64-sided polygon, solve the integral in (24) analytically for each side, and then sum the contributions to obtain the induced electric field.

TABLE I

E_{Na}	Sodium Nernst potential	50.0 mV
E_K	Potassium Nernst potential	−77.0 mV
E_L	Leakage Nernst potential	−54.387 mV
g_{Na}	Sodium conductance	120.0 mmho/cm^2
g_K	Potassium conductance	36.0 mmho/cm^2
g_l	Leakage conductance	0.3 mmho/cm^2
C_m	Membrane capacitance	1.0 μF/cm^2
R_i	Resistivity of axoplasm	0.0354 kΩ · cm
a	Fiber radius	0.0238 cm

Equation (24) determines the electric field produced by electromagnetic induction. In general there can be an additional contribution to the electric field due to a charge distribution [16]. In an *in vitro* experiment where the coil lies in a plane parallel to the air-bath interface no charge accumulates, so the electric field due to charge vanishes and (24) correctly predicts the total electric field. If the coil does not lie parallel to the bath surface, or if the nerve lies inside tissue with a complicated geometry and inhomogeneous electrical properties (such as a human limb), then accumulation of charge on the tissue–air interface or at the boundary between two tissues with different conductivities may contribute significantly to the total electric field [24]. This contribution could be incorporated into our model by adding a term like that proposed by Rattay [14]. Furthermore, the electric field along a fiber may be influenced by its position within a nerve bundle [25], [26]. In this paper we neglect these effects and assume that (24) correctly gives the electric field at the position of the nerve. Simulation of *in vivo* nerve stimulation requires consideration of the influence of tissue conductivity and geometry on the electric field.

When considering the stimulation of a specific nerve, the position and orientation of the coil relative to the fiber must be prescribed. We position the center of the coil at the origin of an x-y coordinate system (Fig. 1), and assume that the plane of the coil lies parallel to and a distance $z = 1$ cm above the nerve. Furthermore, we take the x-axis to be parallel to the nerve and assume that the nerve is tangent to the coil at $y = r_c$.

The x component of the electric field as a function of x and y is shown in Fig. 3(a) for one instant in time ($dI/dt = 1$ A/μs). The bold line at $y = r_c$ denotes the position of the nerve, and the circle projected into the x-y plane indicates the position of the coil. Figure 3(b) shows the x derivative of this component of the electric field, which depends in a complex way on position; its maximum is not below the center of the coil nor at its edge. This spa-

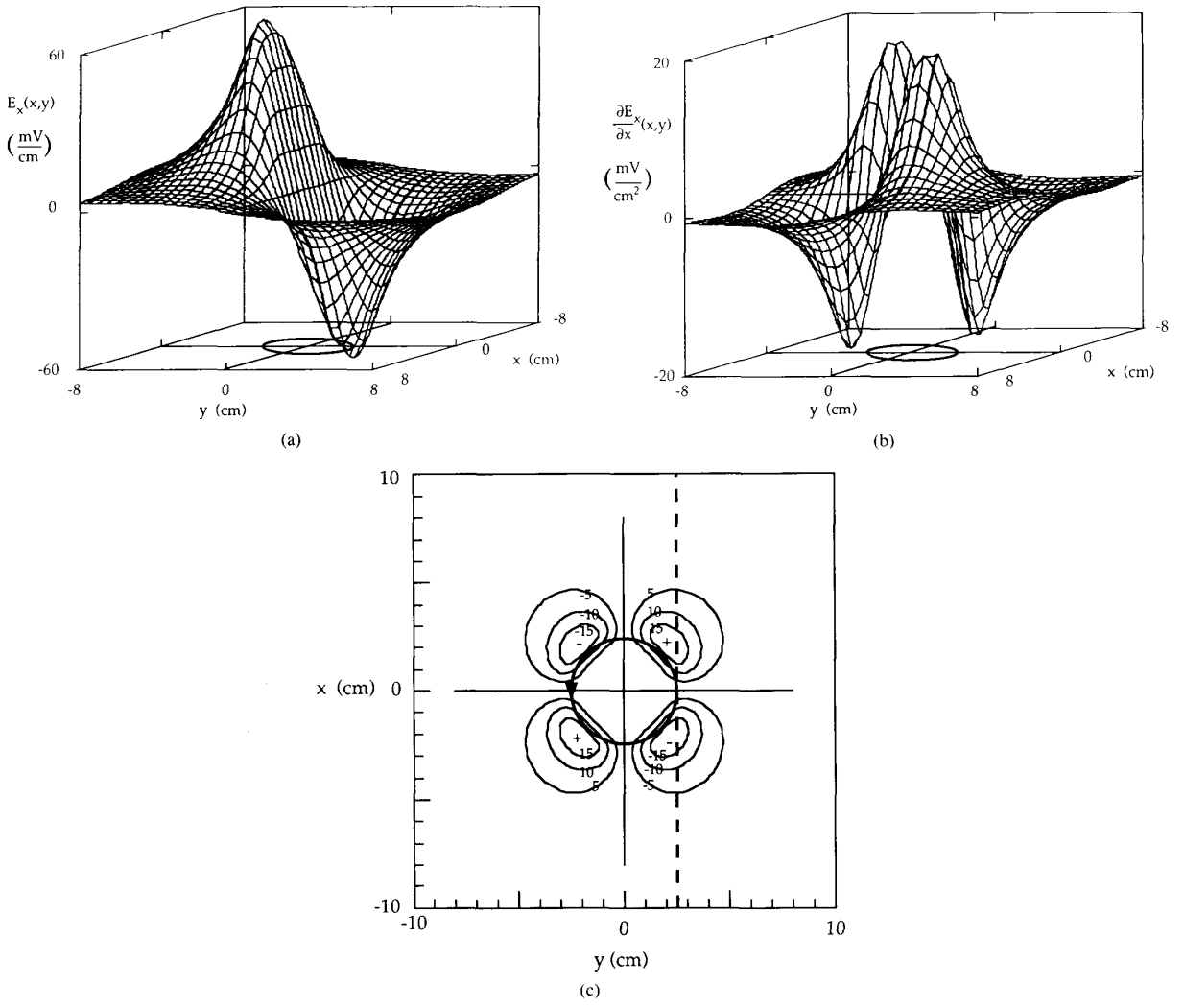

Fig. 3. (a) The x component of the induced electric field ϵ_x as function of x and y, calculated in a plane 1.0 cm below a circular coil whose radius r_c is 2.5 cm. (b) The axial (x) derivative of the x component of the electric field, $\partial\epsilon_x/\partial x$, as function of x and y. (c) A contour plot of $\partial\epsilon_x/\partial x$ as a function of x and y, with each curve representing increments of 5 mV/cm^2. The bold circle represents the position of the coil and the dashed line the position of the nerve. The minus sign indicates the location where a nerve lying parallel to the x axis will be maximally depolarized; the plus sign indicates the position of maximum hyperpolarization.

tial distribution has an unexpected influence on the location of stimulation. Fig. 3(c) shows a contour plot of $\partial\epsilon_x/\partial x$ as a function of x and y. The bold circle represents the position of the coil, with the arrowhead pointing in the direction of the rate of change of the current (the direction of the current when the current is increasing in time), and the dotted line indicates the location of the nerve fiber. The minus signs indicate the regions where we expect a nerve that is parallel to the x axis to be maximally depolarized, i.e., the location of stimulation. The plus signs indicate areas of hyperpolarization.

The Current in the Coil

The coil current $I(t)$ is predicted by a series RLC model of the current stimulator [27] (Fig. 4). The current pulse is generated when a capacitor C, initially charged to a voltage V_o, is discharged through a coil whose inductance is L and resistance is R. In practice the circuit that generates the current pulse may be more complex than the one we use. For example, it may contain several capacitors wired in parallel [28], [29], a transformer to increase the current in the coil [30], or nonlinear elements such as

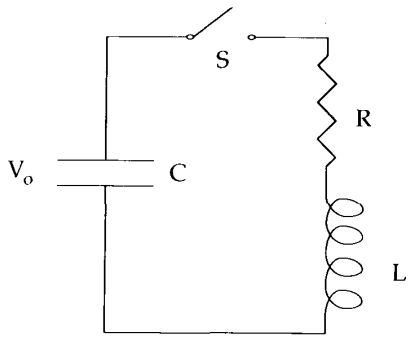

Fig. 4. An RLC circuit used to represent the stimulating circuit. The capacitor C is charged to an initial voltage V_o. At time $t = 0$ the switch S is closed and the capacitor is discharged through the coil inductance L and resistance R.

diodes to reduce oscillations [1], [6], [31], [32]. We chose the series RLC circuit because it is the simplest model of a stimulator that produces realistic current waveforms. However, more complicated circuits whose current waveforms could be calculated analytically or numerically could easily be incorporated into this model.

The inductance L of a circular coil of radius r_c wound with N turns of wire having radius r_w is [33]

$$L = \mu_0 r_c N^2 \left(\ln\left(\frac{8r_c}{r_w}\right) - 1.75 \right). \quad (25)$$

A coil of radius 2.5 cm with 30 turns wound from 1.0 mm radius wire has an inductance of 0.165 mH. Using this value of L, and given values of C, R, and V_o, we can calculate the coil current $I(t)$ from elementary circuit theory. The current either rises to a maximum and then falls to zero (overdamped), or else it oscillates with decreasing amplitude (underdamped), depending whether $R^2/(4L^2) - 1/(LC)$ is greater than or less than zero, respectively [34]. The critically damped case ($R^2/(4L^2) - 1/(LC) = 0$) is difficult to achieve experimentally and will not be considered here. If the circuit is overdamped, the current is given by the following expression:

$$I(t) = V_o C \omega_2 e^{-\omega_1 t} \left(\left(\frac{\omega_1}{\omega_2}\right)^2 - 1 \right) \sinh(\omega_2 t) \quad (26)$$

where

$$\omega_1 = \frac{R}{2L} \quad (27)$$

and

$$\omega_2 = \sqrt{\left(\frac{R}{2L}\right)^2 - \frac{1}{LC}}. \quad (28)$$

If the current is underdamped, then

$$I(t) = V_o C \omega_2 e^{-\omega_1 t} \left(\left(\frac{\omega_1}{\omega_2}\right)^2 + 1 \right) \sin(\omega_2 t), \quad (29)$$

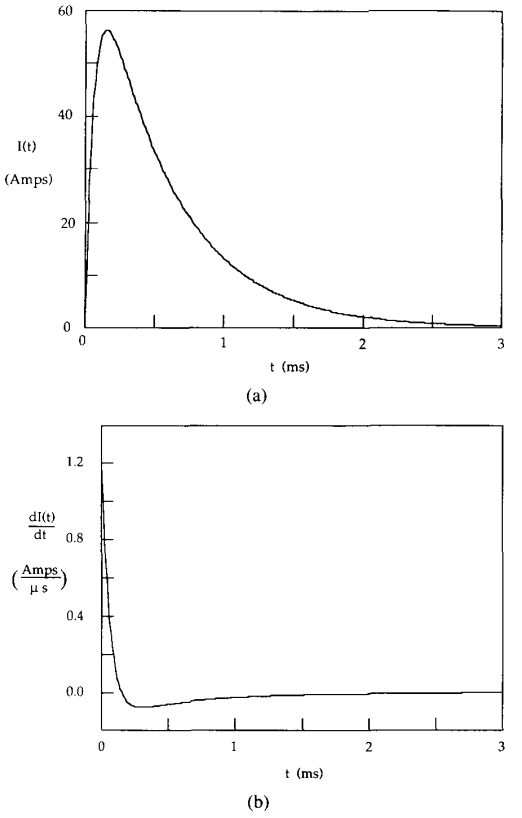

Fig. 5. The time course of (a) the current stimulus $I(t)$ and (b) its time derivative. This waveform was generated using (26), with $R = 3\ \Omega$, $L = 0.165$ mH, and $C = 200\ \mu$F, selected to approximate the current pulse given by Hess *et al.* [7].

where ω_1 is the same as given above and

$$\omega_2 = \sqrt{\frac{1}{LC} - \left(\frac{R}{2L}\right)^2}. \quad (30)$$

Assuming that $C = 200\ \mu$F and $R = 3.0\ \Omega$, we find that the circuit is overdamped with $\omega_1 = 9.07\ \text{ms}^{-1}$ and $\omega_2 = 7.21\ \text{ms}^{-1}$. The resulting current waveform is shown in Fig. 5(a), with $V_o = 200$ V. Its time derivative, given in Fig. 5(b), is bipolar. Using a current pulse that rises and falls we cannot produce a monopolar stimulation pulse, as is often used in electrical stimulation (dI/dt would exhibit multiple zero-crossings if the coil current were oscillating). We can, however, adjust the resistance and capacitance so that current rises faster than it falls. We chose C and R so that our current waveform approximates that given by Hess *et al.* [7].

To obtain the electric field gradient $\partial \epsilon_x(x, t)/\partial x$ we simply modulate the function of space in Fig. 3(b) (along the line $y = r_c$) by the function of time in Fig. 5(b). This product is the source of transmembrane potential which acts to stimulate the nerve. Fig. 6 shows a three-dimensional plot of the induced electric field gradient as a function of time and distance along the fiber.

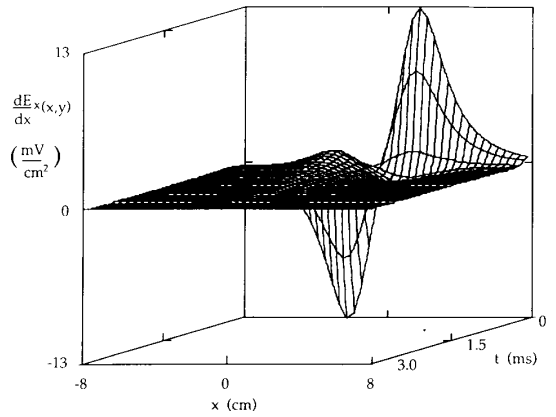

Fig. 6. The source term $\partial\epsilon_x/\partial x$ as a function of x and t, evaluated along the length of the nerve fiber. This function represents the gradient of the electric field along the line $y = r_c$, shown in Fig. 3(b), modulated in time by the current waveform shown in Fig. 5(b).

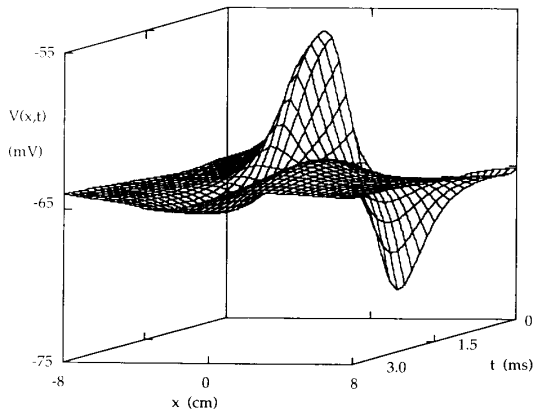

Fig. 7. A three-dimensional plot of the subthreshold response of the nerve fiber to electromagnetic stimulation (V_o = 30 V). The vertical axis is the transmembrane potential in the fiber, and the horizontal axes represent the distance along the fiber x and the time after the capacitor was discharged t.

Results

The model is used to determine the response of the nerve fiber to current pulses of different amplitudes. If the stimulus strength is below threshold, e.g., V_o = 30 V, the fiber behaves like a passive cable and the induced voltage is dissipated. Fig. 7 shows a three-dimensional plot of the subthreshold transmembrane potential as a function of distance along the fiber and elapsed time since the pulse is applied. Direct comparison of Figs. 6 and 7 show that the resulting transmembrane potential has a time course that resembles the time course of the electric field, although the response of the nerve is somewhat delayed due to the time required for the accumulation of charge on the membrane.

If the stimulus strength is slightly larger (V_o = 32.5 V), an action potential is evoked. The three-dimensional plot [Fig. 8(a)] shows the depolarized portion of the nerve has been stimulated, while the hyperpolarized portion is not. After a latency period of about 1.0 ms, the transmembrane potential is seen to rise rapidly, producing two action potentials which propagate in opposite directions along the nerve. The contour plot [Fig. 8(b)] clearly shows the speed of the wave, the latency period, and the site of stimulation. The action potential is initiated at $x = -2.0$ cm, which corresponds to the position of the maximum of $-\partial\epsilon_x/\partial x$, as shown in Fig. 6.

For larger stimuli, e.g., V_o = 150 V, more complicated dynamics are observed. Fig. 9(a) shows two action potentials, traveling in opposite directions, that are evoked after a much shorter latency period. Fig. 9(b) shows that a region of several centimeters along the fiber was simultaneously brought above threshold, so it is difficult to define the exact location of stimulation. The resulting wave traveling in the positive x direction through the hyperpolarized region propagates more slowly than the wave traveling in the negative x direction through the depolarized region.

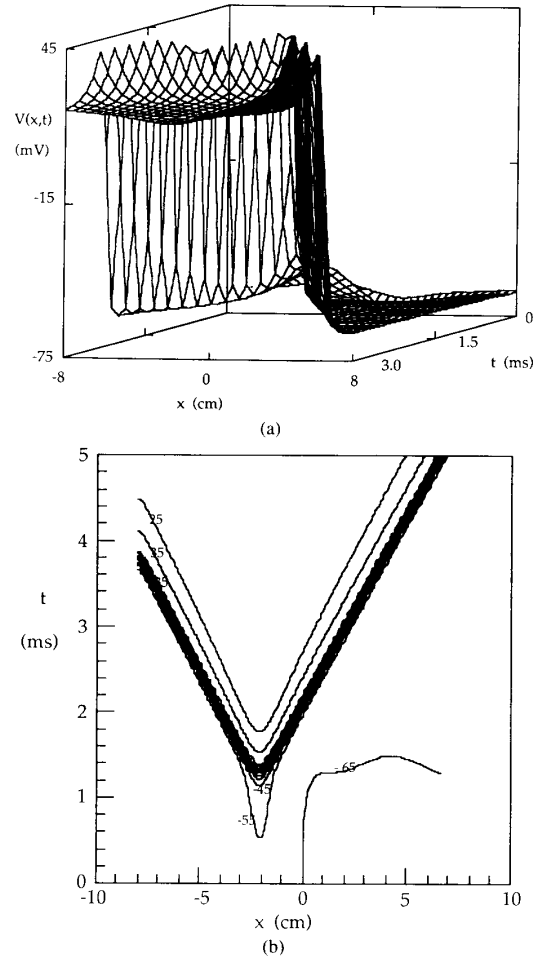

Fig. 8. (a) A three-dimensional plot of the response of the nerve fiber to electromagnetic stimulation just above threshold (V_o = 32.5 V). The vertical axis is the transmembrane potential, and the horizontal axes represent the distance along the fiber x and the time after the capacitor is discharged t. (b) The same function in a contour plot.

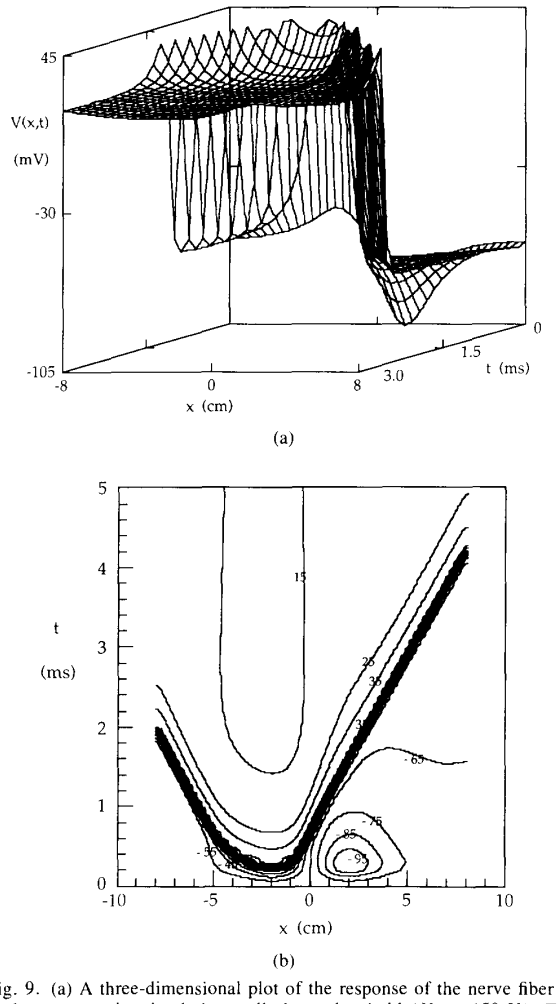

Fig. 9. (a) A three-dimensional plot of the response of the nerve fiber to electromagnetic stimulation well above threshold (V_o = 150 V). The vertical axis is the transmembrane potential in the fiber, and the horizontal axes represent the distance along the fiber x and the time after the capacitor is discharged t. (b) The same function in a contour plot.

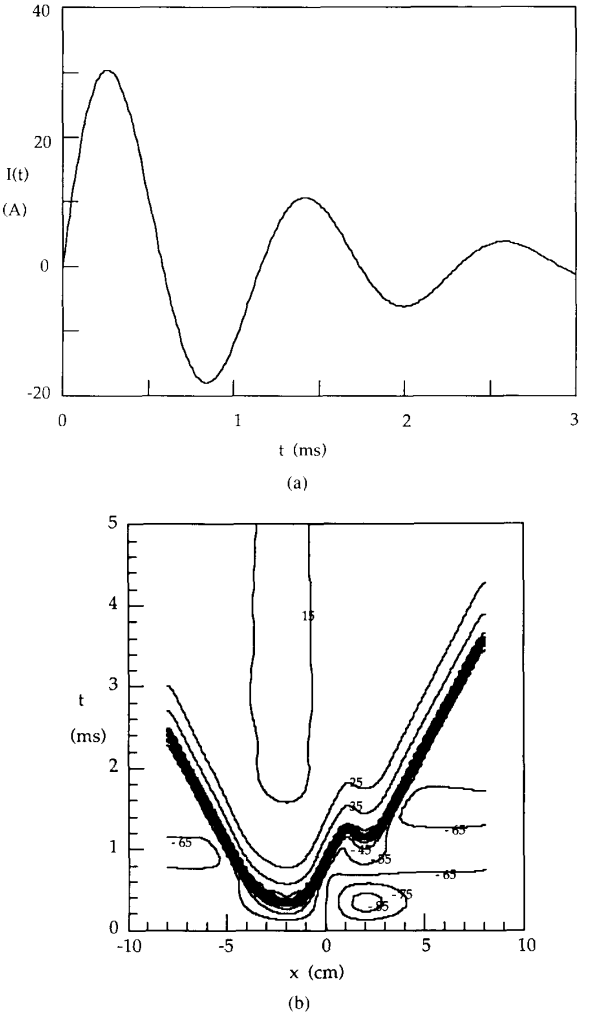

Fig. 10. (a) The coil current as a function of time for R = 0.3 Ω (V_o = 35 V). (b) A contour plot of the transmembrane potential as a function of distance along the fiber x and time after the capacitor is discharged t.

We can change the time course of the stimulus pulse by reducing the resistance of the stimulating circuit to 0.3 Ω, making the current waveform underdamped so that the current oscillates several times before decaying to zero [Fig. 10(a)]. Such oscillations give rise to even more complicated dynamics, shown in the contour plot of the transmembrane potential in Fig. 10(b) (V_o = 35 V). Two action potentials are initiated at $x = -2.0$ cm after a latency of only 0.4 ms. Before the right-going front propagates past the right edge of the coil, the derivative of the current in the coil has already changed sign there, depolarizing the nerve at $x = +2.0$ cm, and initiating two more action potentials. The two action potentials that are propagating towards each other collide and annihilate one another. The remaining two action potentials propagate away from each other, having different apparent latency periods and origins of stimulation. It is not necessary to have an underdamped circuit in order to observe such behavior; we have seen these effects with overdamped circuits for fibers with different conduction velocities or coils with a larger diameter. With more elaborate coil designs, electromagnetic stimulation may give rise to phenomena such as conduction blockage at large stimulus strengths, similar to that observed by Rattay [19] in electrical stimulation.

Discussion

The relationship between the location of stimulation and the position and orientation of the coil relative to the nerve is not simple. For any given coil and a specified direction for the nerve fibers, we can use our model to determine a "volume of stimulation," for which only fibers passing through this volume are stimulated [19]. The edge of this volume might be called the "virtual cathode" associated with stimulation by electromagnetic induction [35]. For

some coil geometries, the shape of the virtual cathode might be very complex.

If we stimulate an action potential once with our coil, then reverse the polarity of the coil current and stimulate again, our model predicts that propagated action potentials measured at a common point far from the stimulating coil differ by a delay due to the change in the location of stimulation [from the $x = -2.0$ cm to $x = +2.0$ cm in Fig. 3(c)]. This theoretical prediction is not consistent with measurements on the human median nerve [10], [36], [37], although in these experiments the coil orientations were somewhat different. More importantly, in this model we have not accounted for the charge accumulation on the surface of the arm, which could significantly affect the electric field distribution along the nerve [24]. It is important that additional experiments and theoretical studies be performed to resolve this issue.

Our model can be used to calculate a strength-duration curve for electromagnetic stimulation for various pulse shapes [27], [34]. In addition, we expect fibers with different diameters or membrane properties to have different stimulus thresholds. This selectivity may differ for myelinated and unmyelinated nerves, and has been shown experimentally to differ for motor and sensory fibers [38].

Another application of this model is in designing stimulator/coil systems. Both the spatial variation of the stimulus and the time course of the current pulse depend on the coil geometry. It is desirable to deliver a focal stimulus. The criterion for designing such a coil is to localize the axial derivative of the axial component of the electric field. The time course of the current pulse depends on the coil inductance. Changes in coil geometry that improve the spatial localization of the stimulus may also influence the temporal characteristics of the current waveform. We have not examined this tradeoff in this paper, but clearly future coil optimization schemes must consider both the temporal and spatial aspects of coil design.

It is difficult to extend this model to describe the stimulation of neurons in the cortex [36]. Because of the small size and complicated geometry of these neurons, we do not know if the conclusions reached in this paper for one-dimensional nerve fibers apply.

Conclusion

We have calculated the response of a nerve fiber to electric fields produced by electromagnetic induction. Three aspects of electromagnetic stimulation are coupled and must be considered together in one model: the current pulse shape, the spatial distribution of the induced electric field, and the interaction of the electric field with the nerve. Our primary conclusion is that the location and timing of the stimulus depend on the axial derivative of the axial component of the induced electric field. The model is useful for the design of optimized coils for stimulating peripheral nerves. However, the extension of the model to account for neurons in the cortex is not obvious.

Acknowledgment

We thank M. Hallett, L. Cohen, W. Friauf, and H. Cascio for useful discussions. We appreciate the efforts of R. Levin, who provided the three-dimensional and contour plotting routines. We also wish to thank B. Dedrick and B. Heetderks for their careful reading of our manuscript.

References

[1] M. J. R. Polson, A. T. Barker, and S. Gardiner, "Stimulation of nerve trunks with time-varying magnetic fields," *Med. Biol. Eng. Comput.*, vol. 20, pp. 243-244, 1982.
[2] A. T. Barker, R. Jalinous, and I. L. Freeston, "Noninvasive magnetic stimulation of human motor cortex," *Lancet*, vol. 1, pp. 1106-1107, 1985.
[3] L. G. Cohen, S. Bandinelli, S. Lelli, and M. Hallett, "Noninvasive mapping of hand motor somatotopic area using magnetic stimulation," *J. Clin. Neurophysiol.*, vol. 5, pp. 371-372, 1988.
[4] L. G. Cohen, S. Lelli, and M. Hallett, "Noninvasive mapping of human motor cortex with magnetic stimulation," *Neurology*, vol. 38 (suppl. 1), pp. 386-387, 1988.
[5] R. Benecke, B.-U. Meyer, P. Schonle, and B. Conrad, "Transcranial magnetic stimulation of the human brain: Responses in muscles supplied by cranial nerves," *Exp. Brain Res.*, vol. 71, pp. 623-632, 1988.
[6] A. T. Barker, I. L. Freeston, R. Jalinous, and J. A. Jarratt, "Magnetic stimulation of the human brain and peripheral nervous system: An introduction and the results of an initial clinical evaluation," *Neurosurgery*, vol. 20, pp. 100-109, 1987.
[7] C. W. Hess, K. R. Mills, and N. M. F. Murray, "Responses in small hand muscles from magnetic stimulation of the human brain," *J. Physiol.*, vol. 388, pp. 397-419, 1987.
[8] K. R. Mills, N. M. F. Murray, and C. W. Hess, "Magnetic and electrical transcranial brain stimulation: Physiological mechanisms and clinical applications," *Neurosurg.*, vol. 20, pp. 164-168, 1987.
[9] D. Claus, A. E. Harding, C. W. Hess, K. R. Mills, N. M. F. Murray, and P. K. Thomas, "Central motor conduction in degenerative ataxic disorders: a magnetic stimulation study," *J. Neurol. Neurosurg. Psychiatry*, vol. 51, pp. 790-795, 1988.
[10] B. A. Evans, W. J. Litchy, and J. R. Daube, "The utility of magnetic stimulation for routine peripheral nerve conduction studies," *Muscle Nerve*, vol. 11, pp. 1074-1078, 1988.
[11] A. L. Hodgkin and W. A. H. Rushton, "The electrical constants of a crustacean nerve fiber," *Proc. Roy. Soc., Ser. B*, vol. 133, pp. 444-479, 1946.
[12] R. Lorente de No, "A study of nerve physiology," *Studies Rockefeller Inst. Med. Res.*, vol. 131-132, 1947.
[13] J. W. Clark and R. Plonsey, "A mathematical evaluation of the core conductor model," *Biophys. J.*, vol. 6, pp. 95-112, 1966.
[14] F. Rattay, "Analysis of models for external stimulation of fibers," *IEEE Trans. Biomed. Eng.*, vol. BME-33, pp. 974-977, 1986.
[15] R. Plonsey, "The active fiber in a volume conductor," *IEEE Trans. Biomed. Eng.*, vol. BME-21, pp. 371-381, 1974.
[16] J. D. Jackson, *Classical Electrodynamics*. New York: Wiley, 1975.
[17] L. G. Cohen, B. J. Roth, J. Nilsson, N. Dang, M. Panizza, S. Bandinelli, W. Friauf, and M. Hallett, "Effect of coil design on delivery of focal magnetic stimulation. I. Technical Considerations," *Electroencephalogr. clin Neurophysiol.*, in press.
[18] W. A. H. Rushton, "Effect upon the threshold for nervous excitation of the length of the nerve exposed and the angle between current and nerve," *J. Physiol.*, vol. 63, pp. 357-377, 1927.
[19] F. Rattay, "Ways to approximate current-distance relations for electrically stimulated fibers," *J. Theor. Biol.*, vol. 125, pp. 339-349, 1987.
[20] F. Rattay, "Modeling the excitation of fibers under surface electrodes," *IEEE Trans. Biomed. Eng.*, vol. BME-35, pp. 199-202, 1988.
[21] J. P. Reilly, "Peripheral nerve stimulation by induced electric currents: exposure to time-varying magnetic fields," *Med. Biol. Eng. Comput.*, vol. 27, pp. 101-110, 1989.

[22] A. L. Hodgkin and A. F. Huxley, "A quantitative description of membrane current and its application to conduction and excitation in nerve," *J. Physiol.*, vol. 117, pp. 500-544, 1952.
[23] R. Plonsey and D. Heppner, "Considerations of quasi-stationarity in electrophysiological systems," *Bull. Math. Biophys.*, vol. 29, pp. 657-664, 1967.
[24] B. J. Roth, L. G. Cohen, M. Hallett, W. Friauf, and P. Basser, "A theoretical calculation of the electric field induced by magnetic stimulation of a peripheral nerve," *Muscle Nerve*, in press.
[25] K. W. Altman and R. Plonsey, "Development of a model for point source electrical fibre bundle stimulation," *Med. Biol. Eng. Comput.*, vol. 26, pp. 466-475, 1988.
[26] P. H. Veltink, J. A. van Alste, and H. B. K. Boom, "Simulation of intrafascicular and extraneural nerve stimulation," *IEEE Trans. Biomed. Eng.*, vol. BME-35, pp. 69-75, 1988.
[27] C. Reuter, J. H. Battocletti, J. Myklebust, and D. Maiman, "Magnetic stimulation of peripheral nerves," presented at IEEE Eng. Med. Biol. Soc. 10th Annu. Internat. Conf., 1988, pp. 928-929.
[28] P. A. Merton and H. B. Morton, "A magnetic stimulator for the human motor cortex," *J. Physiol.*, vol. 381, p. 10P, 1986.
[29] P. O. Byrne, J. A. Eyre, B. R. Kenyon, T. H. H. G. Koh, S. Miller, and P. D. Oliver, "High-current discharge circuit for electromagnetic stimulation of the brain in man," *J. Physiol.*, vol. 391, p. 3P, 1987.
[30] D. Cohen, "Feasibility of a magnetic stimulator for the brain," in *Biomagnetism: Applications and Theory*, Weinberg, Stroink and Katila, Eds. New York: Pergamon, 1985, pp. 466-470.
[31] R. G. Bickford, M. Guidi, P. Fortesque, and M. Swenson, "Magnetic stimulation of human peripheral nerve and brain: Response enhancement by combined magnetoelectrical technique," *Neurosurg.*, vol. 20, pp. 110-116, 1987.
[32] K. Davey, K. C. Kalaitzakis, and C. Epstein, "Transcranial magnetic stimulation of the cerebral cortex," presented at IEEE Eng. Med. Biol. Soc. 10th Annu. Internat. Conf., 1988, pp. 922-923.
[33] W. R. Smythe, *Static and Dynamic Electricity.* New York: McGraw-Hill, 1968.
[34] L. A. Geddes, "Optimal stimulus duration for extracranial cortical stimulation," *Neurosurg.*, vol. 20, pp. 94-99, 1988.
[35] W. C. Wiederholt, "Stimulus intensity and site of excitation in human median nerve sensory fibers," *J. Neurol. Neurosurg. Psychiatry*, vol. 33, pp. 438-441, 1970.
[36] V. E. Amassian, R. Q. Cracco, and P. J. Maccabee, "Basic mechanisms of magnetic coil excitation of nervous system in humans and monkeys and their applications," presented at Special Symp. Maturing Technologies and Emerging Horizons, 1988, pp. 10-17.
[37] P. J. Maccabee, V. E. Amassian, R. Q. Cracco, and J. A. Cadwell, "An analysis of peripheral motor nerve stimulation in humans using the magnetic coil," *Electroencephalogr. clin. Neurophysiol.*, vol. 70, pp. 524-533, 1988.
[38] M. Panizza, J. Nilsson, and M. Hallett, "Relevance of stimulus duration for activation of motor and sensory fibers: Implications for the study of H-reflexes and magnetic stimulation," *J. Clin. Neurophysiol.*, vol. 5, p. 372, 1988.

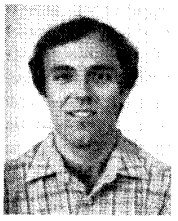

Bradley J. Roth was born in Clinton, IA, in 1960. He received the B.S. degree in physics in 1982 from the University of Kansas, Lawrence, and the Ph.D. degree in physics in 1987 from Vanderbilt University, Nashville, TN.

He is presently a Staff Fellow with the Biomedical Engineering and Instrumentation Branch at the National Institutes of Health, Bethesda, MD. His current research interests are the measurement and modeling of biomagnetic fields, the stimulation of nerves by electromagnetic induction, and the electrical properties of multicellular tissues.

Peter J. Basser was born in New York in 1957. He received the S.M. and Ph.D. degrees in engineering sciences from Harvard University, Boston, MA, in 1982 and 1986, respectively.

He is presently a Staff Fellow in the Biomedical Engineering and Instrumentation Branch of the National Institutes of Health, Bethesda, MD. His current research interests include developing biomimetic sensors and actuators, noninvasive methods to stimulate excitable tissue, and continuum mechanical models of biological tissue.